Results in Physics 23 (2021) 104021

Contents lists available at ScienceDirect

Results in Physics

journal homepage: www.elsevier.com/locate/rinp

Numerical design of high-performance WS_2/metal/WS_2/graphene heterostructure based surface plasmon resonance refractive index sensor

Biswajit Dey [a], Md. Sherajul Islam [a,*], Jeongwon Park [b,c]

[a] Department of Electrical and Electronic Engineering, Khulna University of Engineering & Technology, Khulna 9203, Bangladesh
[b] School of Electrical Engineering and Computer Science, University of Ottawa, Ottawa, ON K1N 6N5, Canada
[c] Department of Electrical and Biomedical Engineering, University of Nevada, Reno, NV 89557, USA

ARTICLE INFO

Keywords:
Surface plasmon resonance
WS2
Metal
WS2 graphene heterostructure
Composite layer sensor

ABSTRACT

The development of a high-performance bio-sensor utilizing the surface plasmon resonance (SPR) phenomenon has attracted great attention recently as a promising and precise sensing technology. Here, we proposed a WS_2/metal/WS_2/graphene heterostructure based SPR sensor with improved performances. The finite-difference time-domain (FDTD) technique was employed to model and develop the prospective sensor. The effects of integrating different layers, the analyte thickness on the performance of the sensor, and the electric field distribution were investigated systematically. We found that the optimized structure of the developed sensor exhibits the highest sensitivity of 208 deg/RIU with a detection accuracy of 1.12 and a quality factor of 223.66 RIU^{-1}, which is superior to existing two-dimensional material based SPR sensors. The enhancement of light-material interaction caused by the coating of a monolayer WS_2 on both sides of the metal improved the sensor performance significantly. These findings demonstrate a new way of performance enhancement in the composite layer sensor, aimed at further improving the identification of specific biomolecules such as glucose, blood disease, environmental monitoring, and agricultural applications.

Introduction

Of late, surface plasmon resonance (SPR) has appealed as one of the most promising sensing techniques due to its key benefits, including a high degree of sensitivity, more user-friendly, lower cost, as well as label-free and real-time identification over conventional biosensors. Such enticing features allow SPR-based sensors desirable for many biosensing applications, including temperature measurement [1], detection of formalin [2], human blood group [3], glucose [4], food and environmental interest [5], gas sensing [6], bacteria [7], urine [8], DNA hybridization [9], living cell analysis [10], etc. However, sensor performance is one of the vital aspects of biological sensing, and exploring the performance enhancement mechanism in SPR biosensors is a research hotspot. In an attempt to optimize the sensor performance, Shalabney et al. [11] suggested a variety of methods, such as optimization of metal layers, the effect of the prism index and dispersion, the addition of nano-dielectric layers, incorporation of the gratings on the top of metals. A bimetallic film was also suggested by Dyankov et al. [12] to enhance the sensitivity of the SPR sensor. In this regard, Kashyap et al.[13] and Chen et al. [14] proposed a bimetallic sensor based on Ag-Au with increased sensitivity and reduced FWHM compared to a single metal-based sensor, providing a high detection accuracy. Nevertheless, the performance of SPR sensors requires further enhancement for practical applications.

Thanks to their remarkable electrical and optical properties, two-dimensional (2D) materials such as graphene and transition metal dichalcogenides (TMDCs) have been used in recent years to build SPR sensors [15]. 2D materials have versatile biocompatibility and a greater adsorption surface area that improves sensor performance and quality [16]. TMDCs induce a strong coupling at the metal/TMDCs interface, which enhances the electric field. The enhanced electrical field is extremely sensitive to the analyte's refractive index shift, resulting in improved sensitivity. Moreover, a larger real part of the dielectric constant of these materials enables the absorption of light energy by metal [17]. The sensitivity of the conventional SPR sensor is not high enough because the metal layer cannot absorb enough light energy for stronger excitation. However, TMDCs can absorb higher light energy due to its large real part of the dielectric constant, which provides stronger excitation. Besides, the metal layer can be covered by TMDCs, which offers better stability for the sensor. With these privileges, various SPR sensors

* Corresponding author.
E-mail address: sheraj_kuet@eee.kuet.ac.bd (Md.S. Islam).

https://doi.org/10.1016/j.rinp.2021.104021
Received 15 November 2020; Received in revised form 29 January 2021; Accepted 27 February 2021
Available online 4 March 2021

have been proposed and investigated using 2D-materials. Wu et al. suggested an extremely sensitive SPR sensor based on graphene, which could improve the sensitivity by 25% [18]. A nanostructured SPR biosensor with enhanced sensitivity based on graphene-MoS_2 was suggested by Zeng et al. [19]. The TMDC/Silicon nano-sized SPR sensor was illustrated by Ouyang et al. [20]. They recorded the sensor's optimum sensitivity was 155.68 deg/RIU with an FWHM of 17.46 deg. The efficiency of the sensor was also improved through black phosphorus (BP). Wu et al. [21] reported a biochemical sensor focused on the heterostructure of BP-graphene-bilayer-WSe_2 and enabled to attain the sensitivity of 279 deg/RIU. Although high sensitivity was achieved, however, the broadening of the SPR spectrum has not been shown. In the MoS_2-graphene-aluminum (Al)-based sensor, the sensitivity of 215 deg/RIU was also recorded when the analyte refractive index is 1.42 [22].

Moreover, recent investigations [22,23] show that the coating of different types of TMDCs on both surfaces of the metal film enhances the sensitivity greatly in the SPR sensor. A maximum sensitivity of 190 deg/RIU was obtained by coating MoS_2 on both surfaces of the metal film. A higher sensitivity of 315 deg/RIU was obtained for seven layers WS_2, which is 3.3 times greater than the conventional Al thin film-based sensor. These studies suggest that graphene and TMDCs are excellent candidates for the sensitivity enhancement of the sensor.

Apart from the 2D materials, prior studies revealed that an introduction of an air gap could significantly enhance sensor performance. For instance, a graphene-based sensor with a high air gap of 23 nm has been proposed by Verma et al. [24] with sensitivity 2.35 times greater than that of without an air gap. Rouf et al. [25] proposed an Ag-Au bimetallic InP-based SPR biosensor with a 15 nm air gap, where they obtained the maximum sensitivity of 70.90 deg/RIU. Very high air gaps of 35 nm, 45 nm, and 55 nm have been proposed for graphene multilayer based SPR biosensor by Maharana et al. [26] with the sensitivity of 39.68 deg/RIU, 34.5 deg/RIU, and 33.42 deg/RIU for the wavelength of 700 nm, 850 nm, and 1000 nm, respectively.

Although the uses of TMDCs as well as the introduction of an air gap improve the sensitivity, the FWHM also increases in TMDCs based sensors, which reduces the sensor resolution. On the other hand, along with the large sensitivity, the narrow FWHM and quality factor (sensitivity/FWHM) are the important criteria to design the sensor with specific applications. To enhance the detection accuracy and quality factor, Bijalwan et al. [27] proposed a nanoribbon of graphene/WSe_2 structure. By optimizing the number of graphene and WSe_2 layers, they revealed that the detection accuracy and quality factor could be enhanced by 0.82 to 0.92 and 164.28 RIU^{-1} to 184.97 RIU^{-1} for graphene nanoribbons whereas 0.81 to 0.90 and 162.5 RIU^{-1} to 181.11 RIU^{-1} for WSe_2 nanoribbons, respectively. They also demonstrated that the FWHM increases with increasing layer numbers. However, increasing the layer numbers reduces the detection accuracy and quality factor. Thus, further research is essential to resolve how the sensor performance can be improved with the minimum TMDC/graphene layers.

In this work, with an intention to improve the sensitivity without costing the detection accuracy and quality factor, we proposed a WS_2/metal/WS_2/graphene heterostructure based SPR sensor. The Finite-difference time-domain (FDTD) technique was employed to model and develop the prospective sensor. Through enhancing light-matter interaction using a 2D WS_2 layer on either side of the metals, the performance of the proposed sensor can be enhanced rather than by optimizing the thickness of the layer. The optimized design of the developed sensor revealed an angular sensitivity of 208 deg/RIU with detection accuracy 1.12 and quality factor 223.66 RIU^{-1}, which outperforms compared to the performance of any conventional configurations.

Materials and sensor design

The proposed SPR sensor is based on the Kretschmann configuration [28] using the heterostructure of 2D materials and thin metal layers. The angular interrogation method was applied to obtain the excitation of surface plasmon polarization (SPP). The p-polarized (TM) light with a wavelength of 633 nm was passed through different layers to obtain attenuated total reflection (ATR), which is reflected on the different layer interfaces and captured by the detector. For a particular incident angle, the wave vector is matched with the surface plasmon wave (SPW), known as SPR, and the corresponding angle is called the SPR angle. Consequently, minimal reflection occurs. Fig. 1 demonstrates the schematic of the proposed sensor. The basic structure of the developed sensor consists of 7th layers. The detailed specification and optimized parameters are illustrated in Table 1. We used CF_2 glass as a prism because the lower refractive index of prism offers high sensitivity [29]. The refractive index for CF_2 glass was determined using the following relation as [30]

$$\eta_{prism}^2 = 1 + \frac{0.5675888\lambda^2}{\lambda^2 - 0.050263605^2} + \frac{0.4710914^2}{\lambda^2 - 0.1003909^2} + \frac{3.8484723^2}{\lambda^2 - 34.0649040^2} \quad (1)$$

Aluminum (Al) was selected as an active metal due to its thinner SPR response. Al refractive index was determined employing the Drude equation as follows [31]:

$$\eta_{Al} = \left[1 - \frac{\lambda^2\lambda_c}{\lambda_p^2(\lambda_c + i\lambda)}\right]^{1/2} \quad (2)$$

where $\lambda_p = 1.0657 \times 10^{-7}$ m and $\lambda_c = 2.4511 \times 10^{-5}$ m. A silver (Ag) layer was deposited on it since the use of a bimetallic structure enhances sensitivity in the SPR sensor highly [13,14]. Besides, Ag has the minimum FWHM [32], which increases the DA and QF. As our main concern in this work is the improvement of DA and QF with improving sensitivity, therefore, we have chosen Al/Ag instead of single plasmonic metal. However, Al and Ag both are chemically unstable and prone to oxidation. To stabilize the sensor, monolayer WS_2 was placed on both sides of the metal so that metal can free from the chemical reaction and a huge amount of light energy can be absorbed. To further increase the sensitivity of the sensor, monolayer graphene was selected owing to its unique optical properties and exotic mechanical flexibility [33]. We determined the refractive index of graphene as [34]

$$\eta_G = 3.0 + \frac{ic\lambda}{3} \quad (3)$$

where $c = 5.446\ \mu m^{-1}$.

All the simulations were performed by the 2D Finite-difference time-domain (FDTD) technique using the Lumerical FDTD simulator (Version: 8.19.1584). Parameter sweep was conducted to attain the capability of the source angle to stimulate SPR mode. An overriding mesh area was taken to push a better mesh step size in the y-direction perpendicular to the metal film. The boundary condition was defined in such a way that the reflection of the outgoing wave was absorbed and inhibited. The most widely used absorbing boundary condition with extremely low local reflection is the perfectly matched layer (PML) [35,36]. The PML is a regime where the reflecting plane wave is polarized at a certain frequency and matches the boundary. The PML is intended to capture the outgoing wave from the active domain of computation without reflecting it back to the field of interest. To better absorb light propagating at broad angles from the usual incidence, the PML profile was set to a "steep angle" in this work.

Although this work proposed a numerical design of SPR sensor based on WS_2/metal/WS_2/graphene hybrid structure. However, our proposed theoretical design can also be experimentally realized. Al and Ag layer can be deposited with the help of the electron beam evaporation or sputtering techniques [37,38]. Graphene/WS_2 can be deposited by the chemical vapor deposition (CVD) technique [39-42].

Performance parameters of the SPR sensor

The performance of the SPR sensor during assessment and sensing is

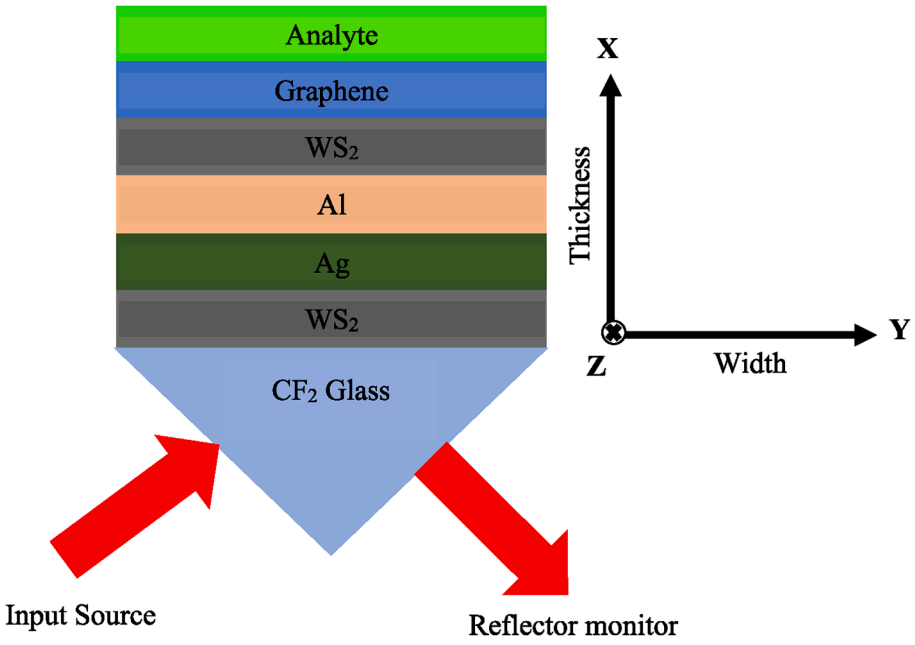

Fig. 1. Schematic diagram of WS_2/metal/WS_2/graphene heterostructure based SPR biosensor.

Table 1
Sensor specification with optimized geometry at 633 nm wavelength.

Layer position	Layer materials	Refractive index (η) [RIU]	Dielectric constant	Thickness, d (nm)
1st Layer	CF_2 glass	1.4329 [30]	2.0532 [30]	———
2rd layer	WS_2	4.8937 + 0.3124i [23]	23.8511 + 3.0578i [23]	0.8 [23]
3th Layer	Ag	0.056206 + 4.2776i [53]	−18.2947 + 0.4809i [53]	20 [optimized]
4th Layer	Al	0.0778 + 5.8535i [31]	−34.2574 + 0.9108i [31]	35 [23]
5th Layer	WS_2	4.8937 + 0.3124i	23.8511 + 3.0578i	0.8
6th Layer	Graphene	3.0 + 1.149106i [23]	7.6796 + 6.8946i [23]	0.34 [23]
7th Layer	Analyte	1.33	———	———

indicated via various parameters. Sensitivity is considered as the main performance parameter, which can be obtained from the ratio of the SPR angle magnitude to the measurand or more specifically the refractive index. Usually, the angle at which minimum reflectivity occurs is indicated as an SPR angle. The slope of the standard graph is connected to this parameter. Generally, sensitivity (S) is formulated using the following relation as [43].

$$S = \frac{\Delta\theta_{SPR}}{\Delta\eta_a}; \text{deg/RIU} \tag{4}$$

where $\Delta\theta_{SPR}$ and $\Delta\eta_a$ represent the change in SPR angle and refractive index of the analyte. The next performance parameter considered in this study is the detection accuracy (DA). This parameter is related to the full width at half maximum (FWHM) of the SPR sensor with the shifting of the SPR angle. The higher the DA, the better the SPR sensor. The DA is formulated as the change in the SPR angle with the spectral width at 50% reflectivity (i.e., FWHM) as [44].

$$DA = \frac{\Delta\theta_{SPR}}{\text{FWHM}}; \tag{5}$$

Another crucial parameter used to characterize the performance of the proposed sensor is the quality factor (QF). The larger QF indicates the better performance of the sensor. The QF is calculated as the ratio of the sensitivity by the spectral width at 50% reflectivity as [23].

$$\text{QF} = \frac{S}{\text{FWHM}}; \text{RIU}^{-1} \tag{6}$$

Results and discussion

At first, we calculated the reflectivity for the various incidence angles generated by the angular integration technique with refractive index $\eta_a = 1.33$ and $\eta_a = 1.335$, considering a 633 nm TM polarized light at the prism-metal surface. Fig. 2a shows the reflection versus SPR angle characteristics of the CF_2/metal structure. The metal film dielectric constant has a significant impact on the SPR parameters. When polarized light strikes on the top of the plasmonic metal through a prism, the light is reflected by the metal film, which acts as a mirror. The polarized light can interact with the free electrons of metal films, generating an oscillation of electrons known as plasmon, thereby decreasing the intensity of the reflected light. For a particular incident angle, the incident light's wave vector is equal to the surface plasmon wave (SPW), inducing an SPR excitation. The minimum reflection occurs at this angle, which is recognized as an SPR angle. Surface plasmon (SP) occurs at the interface of two materials where there is a different sign in the real part of the dielectric function. It is only possible in certain ranges of thickness of the metal film. The basic concept is that SPs are highly sensitive to any changes in the metal surface dielectric environment. Therefore, any slight variation in the refractive index causes a large variation in the SPR parameter. As a result, the SPR angle changes with the variation of the refractive index.

As Fig. 2a suggests, with the increase of the refractive index of the sensing medium, the SPR angle shifts to the right as well as the percentage of reflection increases. This phenomenon can be elucidated via the following relation [45]

$$\theta_{\text{SPR}} = \sin^{-1}\frac{\eta_{eff}\eta_a}{\eta_p\sqrt{\eta_{eff}{}^2 + \eta_a{}^2}} \tag{7}$$

here, η_p and η_a represent the refractive index of the CF_2 glass prism and the analyte, respectively. η_{eff} is the equivalent refractive index (RI) of

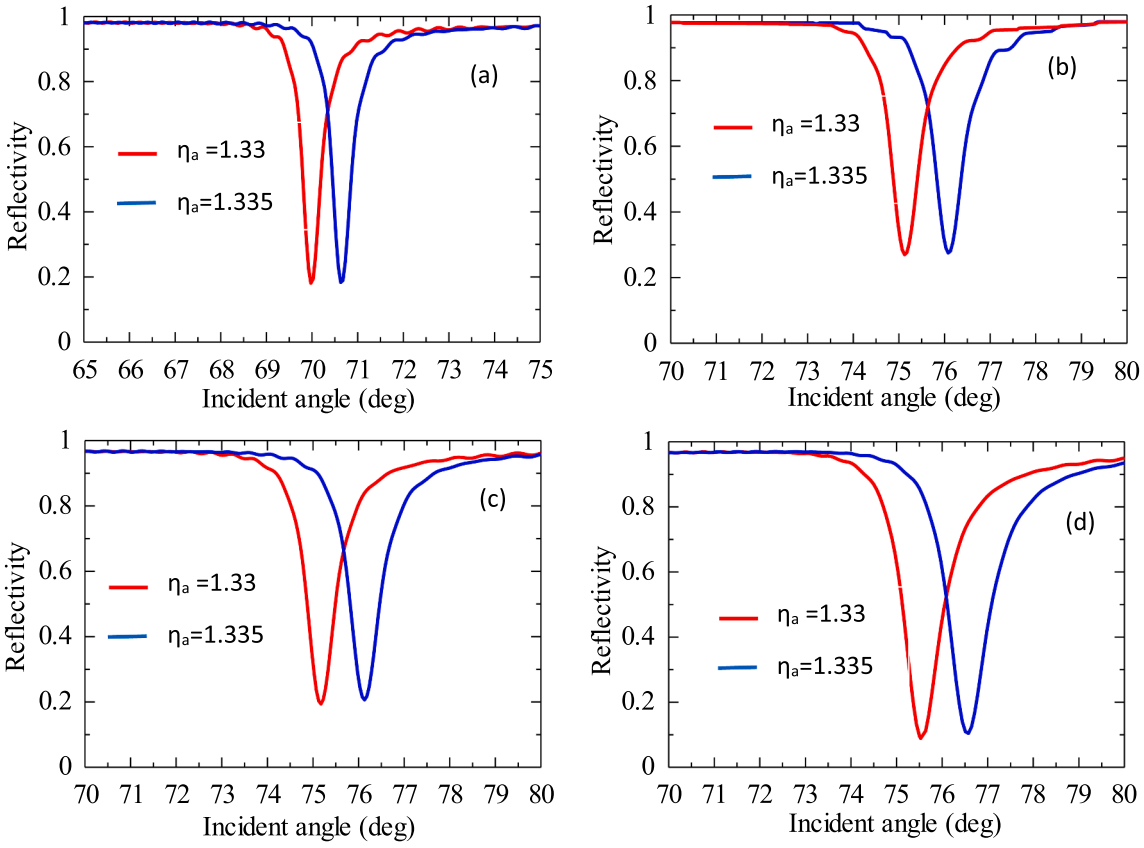

Fig. 2. Sensor response curve (a) without air gap, WS_2 and graphene layer, (b) with WS_2 and without air gap and graphene layer, (c) with WS_2 and graphene layer and without air gap and (d) with air gap, WS_2 and graphene layer.

composite layers. From this equation, it is seen that the SPR angle depends on the η_a. Therefore, with an increasing refractive index of the analyte, the SPR angle is shifted to the right. The obtained SPR angles were 69.97 deg at $\eta_a = 1.33$ and 70.63 deg at $\eta_a = 1.335$. All the performance parameters of the sensor are proportional to the SPR shift. Due to the large shift of the SPR angle as well as the narrower FWHM (0.39 deg), the performance of the SPR sensor increases. The sensitivity, DA, and QF of the sensor were found as 132 deg/RIU, 1.69, and 338.46 RIU^{-1}, respectively. However, the sensitivity is not good enough and further improvement is required. Therefore, a monolayer WS_2 has been proposed to enhance sensor performance. Fig. 2b shows the sensor response curve after adding WS_2 monolayer on both sides of the metal. The SPR angle is changed from 75.13 deg to 76.07 deg, offering enhanced sensitivity (188 deg/RIU). However, the FWHM increases from 0.39 to 0.52 deg. Generally, the enhancing effect produced by WS_2 is associated with its dielectric constant. As can be perceived from Table 1, the WS_2 layer offers a higher real part of the dielectric constant, which provides a strong absorption ability [19,23], resulting in increased sensitivity. It can be explained by the following relation [19]

$$k_{sp} = Re\left[k_0\left(\frac{\varepsilon_{mw}n_a^2}{\varepsilon_{mw}+n_a^2}\right)^{1/2}\right] \tag{8}$$

where, k_0 is the wave vector of the incident light, ε_{mw} is the dielectric constant of the WS_2 enhanced the metallic thin film, and n_a is the refractive index of the analyte. According to Eq. (8), the SP wave vector (k_{sp}) increases due to a larger real part of the dielectric constant, resulting in a larger incident angle requirement for the SP excitation. Besides, k_{sp} also increases with the increase of the analyte's refractive index. Therefore, with a small increase of n_a of the analyte, the value of k_{sp} also increases, resulting in k_{sp} is matched with k_0 at a larger incident angle leading to greater sensitivity. On the other hand, a large broadening is observed in the SPR curve due to the loss of electron energy related to the imaginary part of the dielectric constant [19]. Thus, to further improve the sensitivity, we selected a graphene layer on the WS_2 layer.

Fig. 2c shows the sensor response curve after adding the graphene layer. We observed that the SPR angle of 75.18 deg at $\eta_a = 1.33$ and 76.14 deg at $\eta_a = 1.335$, resulting in an SPR shift of 0.96 deg, which enhances the sensitivity to 192 deg/RIU. Similar to WS_2, graphene has also an imaginary part of the dielectric constant, which broadens the FWHM (0.61 deg). To further improve the performance, an air gap is introduced between the prism and WS_2 layer. Introducing an air gap, the sensor response curve is shown in Fig. 2d. The sensitivity, DA, and QF of the sensor were obtained as 208 deg/RIU, 1.12, and 223.66 RIU^{-1}, respectively, which is far better than the existing 2D materials based SPR sensors. Recent studies [23,27] show that the increasing number of TMDC and graphene layers provide better absorption, resulting in higher sensitivity with increasing FWHM due to higher electron energy loss. Nonetheless, the FWHM of the SPR reflection spectrum is also a crucial parameter along with the sensitivity that must be considered when designing a sensor. Thus, the impact of WS_2 and graphene layer numbers on sensor performance is ignored in this study.

To obtain the optimal thickness of different layers, especially the thickness of metal and air gap at which the maximum performance occurs, we have calculated the thickness dependence of the sensor performance. Considering the Al layer thickness as 35 nm [23], we have optimized the thickness of the Ag layer and the air gap. Fig. 3a shows the sensitivity of the proposed sensor as a function of the Ag thickness without any air gap. The maximum sensitivity was found at the 20 nm thick Ag layer. A further increase in the Ag layer thickness reduces the sensitivity of the sensor, as shown in Fig. 3a. Assuming the optimized thickness of the Ag layer as 20 nm, the performance of the sensor as a function of the air gap thickness is presented in Fig. 3b. As Fig. 3b

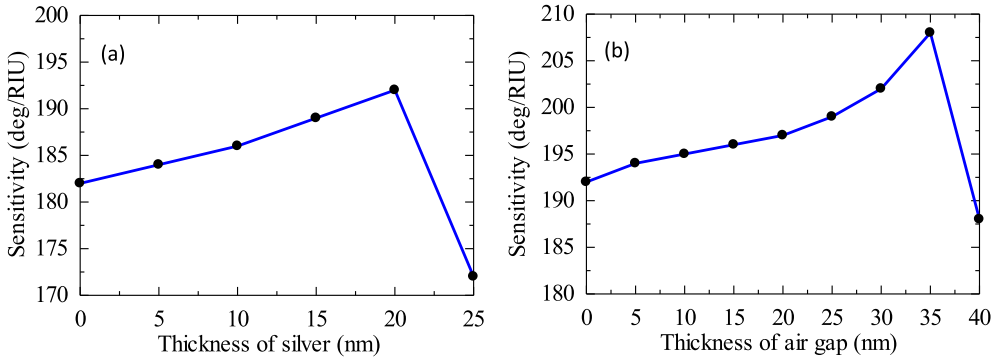

Fig. 3. Thickness dependent sensor performances. The variation of sensitivity as a function of thickness of (a) silver and (b) air gap.

suggests, the highest sensitivity was achieved with an air gap thickness of 35 nm. The sensitivity starts to decrease as the air gap thickness increases more. Hence, the optimized thickness of the Ag and the air gap is determined as 20 nm and 35 nm, respectively.

To further analyze the sensor performance, the refractive index shift caused by the analyte is applied for a finite thickness. Under the optimized design condition, the sensor performance by varying the thickness of the analyte (50 nm-300 nm) is shown in Fig. 4. Although the sensitivity, DA, and QF all were found to increase with the increase in analyte thickness, the sensor still offers good performance at a lower analyte thickness. Even with a 50 nm thin analyte, the sensitivity, DA, and QF were still found to be as high as 26 deg/RIU, 0.43, and 86.67 RIU^{-1}, respectively. The dynamic range of the proposed sensor was also analyzed. We have calculated the SPR angle for different refractive indices of the analyte which are plotted in Fig. 5. The angular response is observed to remain linear in the refractive index range of 1.33–1.36, indicating that any changes in this region can be detected.

For benchmarking, we also analyze the distribution of the electric field of the proposed sensor using the FDTD technique. A 633 nm plane wave TM polarized light source was considered to perform the calculation. Maxwell's equation can be solved easily via the YEE algorithms in the FDTD, which makes it a versatile tool. Compared to other methods such as Green's dynamic technique to resolve Maxwell's equations for complex geometries and dispersive media [46], the FDTD technique provides more accurate results. The PML was used for boundary conditions to enable the waves to reach layers with minimal reflections (R_{min}), and the electric field intensity was monitored using the DFT monitor. The distribution of the electric field in the proposed biosensor is depicted in Fig. 6. It can be perceived that the intensity of the electric field is different for different layers. The electric field strength reaches its optimum value if the reflectance curve shows the lowest reflectivity value. Maximum electric field intensity is obtained in the Al/WS_2/

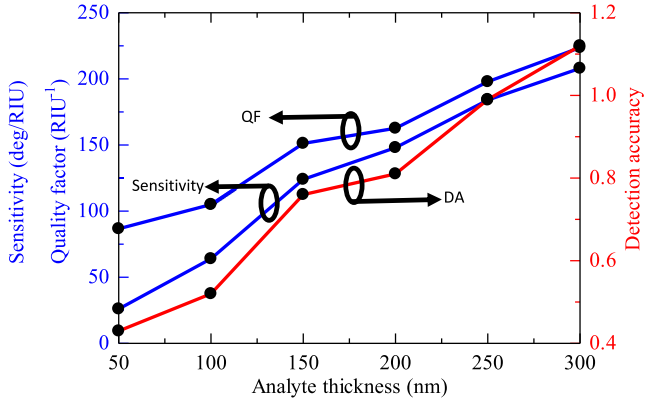

Fig. 4. Sensing medium thickness dependent sensor performances. The sensitivity, detection accuracy and quality factor as a function of analyte thickness.

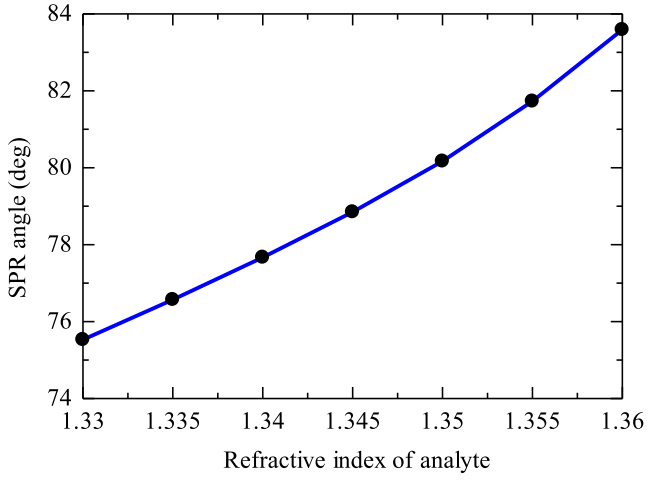

Fig. 5. Variation of SPR angle as a function of analyte refractive index.

graphene layer. It can be said that minimum reflection occurs in the metal layer in surface plasmon conditions. The incorporation of WS_2 layers on the metal film induces a strong coupling at the metal/WS_2 interface owing to the effective charge transfer. This effect greatly enhances the electric field at the sensing inter-face [47-52]. Consequently, an ultra-high sensitivity is perceived. Moreover, the use of WS_2/graphene heterostructure increases the adsorption surface area due to van der Waals force of attraction and enhances the interface field, resulting in a further enhancement of sensitivity. In addition, the air gap in the proposed structure acts as a dielectric medium that increases the reflection spectrum's resonance dip, resulting in an enhanced sensitivity. Besides, the probing field intensity decays exponentially to the analyte with a penetration depth of about 247 nm and the propagation length of about 198 nm. This indicates that the probing electric field near the sensing interface is very strong and would be highly sensitive to the interactions of small biomolecules.

A comparison has also been made between the proposed sensor and the existing 2D materials-based sensors. Table 2 represents the performances of the proposed sensor along with some existing 2D materials-based sensors designed in the earlier works. From the comparison table, it can be observed that the TMDC/graphene heterostructure-based sensor shows the highest sensitivity (315.52 deg/RIU) but very poor QF (18.84 RIU^{-1}). On the other hand, the sensor based on WSe_2 and graphene nanoribbons improved the DA to 0.9 and 0.92 as well as the QF 181.11 RIU^{-1} and 184.97 RIU^{-1}, respectively by the costing of sensitivity. This indicates that the overall performances of the reported sensors still need to be improved. On the other hand, the obtained performance (sensitivity = 208 deg/RIU, DA = 1.12, and QF = 223.66 RIU^{-1}) of the proposed sensor is much better than the existing 2D

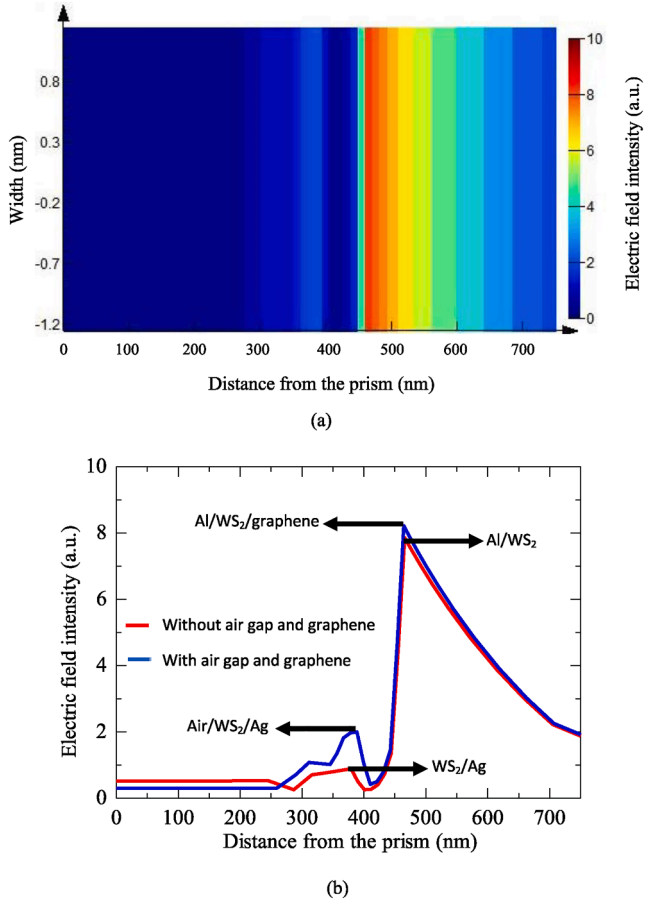

Fig. 6. (a) The electric field distribution at resonance angle 75.53 deg (b) Evanescent field along the direction perpendicular to the prism with and without air gap as well as graphene layer.

Table 2
Comparison of the performances of the proposed sensor to other existing sensors.

Structure	Sensitivity (deg/RIU)	Detection Accuracy	Quality Factor (RIU^{-1})	Reference
Mono layer of Tungsten Disulfide (WS_2) and six layers of Al_2O_3	227.5	1.1123	28.26	[54]
TMDC/Si nanostructure	155.68	.....	9.0	[20]
TMDC/graphene heterostructure	315.52	.....	18.84	[23]
Graphene nano-ribbons	160	0.92	184.97	[27]
WSe_2 nano-ribbons	163	0.9	181.11	[27]
WS_2/Metal/WS_2/Graphene	208	1.12	223.66	Present work

materials-based sensors.

Conclusions

In summary, we systematically modeled a WS_2/metal/WS_2/graphene heterostructure based SPR biosensor with improved performances employing the finite-difference time-domain (FDTD) technique. The effect of adding different layers, the thickness of the analyte on the sensor performance, and the electric field distribution have been investigated thoroughly to attain the optimal performance of the proposed sensor. The optimized structure of the designed sensor revealed a maximum detection accuracy of 1.12, a quality factor of 223.66 RIU^{-1}, and a sensitivity of 208 deg/RIU. The obtained performance is higher compared to the existing 2D materials based SPR sensor. The coating of a monolayer WS_2 on both sides of the metal enhances the light-matter-interaction greatly, which causes a significant improvement of the sensor performance. The proposed biosensor can be a promising candidate for high-performance bio-sensing in medical diagnostic, agricultural applications, and environmental detection.

Funding

This research did not receive any specific grant from funding agencies in the public, commercial, or not-for-profit sectors.

Data availability

The data that support the findings of this study are available from the corresponding author upon reasonable request.

CRediT authorship contribution statement

Biswajit Dey: Conceptualization, Methodology, Software, Data curation. **Md. Sherajul Islam:** Writing - original draft, Visualization, Investigation, Supervision, Software, Validation. **Jeongwon Park:** Writing - review & editing.

Declaration of Competing Interest

The authors declare that they have no known competing financial interests or personal relationships that could have appeared to influence the work reported in this paper.

References

[1] Mollah MdA, Islam SMR, Yousufali Md, Abdulrazak LF, Hossain MbB, Amiri IS. Plasmonic temperature sensor using D-shaped photonic crystal fiber. Results in Physics 2020;16:102966. 10.1016/j.rinp.2020.102966.
[2] Moznuzzaman Md, Rafiqul Islam Md, Biplob Hossain Md, Mustafa Mehedi I. Modeling of highly improved SPR sensor for formalin detection. Results Phys 2020; 16:102874. 10.1016/j.rinp.2019.102874.
[3] Sharma AK, Jha R, Pattanaik HS. Design considerations for surface plasmon resonance based detection of human blood group in near infrared. J Appl Phys 2010;107:034701. https://doi.org/10.1063/1.3298503.
[4] Lam WW, Chu LH, Wong CL, Zhang YT. A surface plasmon resonance system for the measurement of glucose in aqueous solution. Sens Actuators, B 2005;105: 138–43. https://doi.org/10.1016/j.snb.2004.04.088.
[5] Shankaran D, Gobi K, Miura N. Recent advancements in surface plasmon resonance immunosensors for detection of small molecules of biomedical, food and environmental interest. Sens Actuators, B 2007;121:158–77. https://doi.org/10.1016/j.snb.2006.09.014.
[6] Mishra SK, Tripathi SN, Choudhary V, Gupta BD. SPR based fibre optic ammonia gas sensor utilizing nanocomposite film of PMMA/reduced graphene oxide prepared by in situ polymerization. Sens Actuators, B 2014;199:190–200. https://doi.org/10.1016/j.snb.2014.03.109.
[7] Maurya JB, Prajapati YK, Tripathi R. Effect of molybdenum disulfide layer on surface plasmon resonance biosensor for the detection of bacteria. Silicon 2018;10: 245–56. https://doi.org/10.1007/s12633-016-9431-y.
[8] Menon PS, Said FA, Mei GS, Berhanuddin DD, Umar AA, Shaari S, et al. Urea and creatinine detection on nano-laminated gold thin film using Kretschmann-based surface plasmon resonance biosensor. PLoS ONE 2018;13:e0201228. https://doi.org/10.1371/journal.pone.0201228.
[9] Rahman MS, Anower MS, Rahman MK, Hasan MR, Hossain MB, Haque MI. Modeling of a highly sensitive MoS2-Graphene hybrid based fiber optic SPR biosensor for sensing DNA hybridization. Optik 2017;140:989–97. https://doi.org/10.1016/j.ijleo.2017.05.001.
[10] Yanase Y, Yoshizaki K, Kimura K, Kawaguchi T, Hide M, Uno S. Development of SPR imaging-impedance sensor for multi-parametric living cell analysis. Sensors 2019;19:2067. https://doi.org/10.3390/s19092067.
[11] Shalabney A, Abdulhalim I. Sensitivity-enhancement methods for surface plasmon sensors: SPR sensors sensitivity enhancement. Laser & Photon Rev 2011;5: 571–606. https://doi.org/10.1002/lpor.201000009.
[12] Dyankov G, Zekriti M, Bousmina M. Dual-mode surface-plasmon sensor based on bimetallic film. Appl Opt 2012;51:2451. https://doi.org/10.1364/AO.51.002451.
[13] Kashyap R, Chakraborty S, Zeng S, Swarnakar S, Kaur S, Doley R, et al. Enhanced biosensing activity of bimetallic surface plasmon resonance sensor. Photonics 2019;6:108. https://doi.org/10.3390/photonics6040108.

[14] Chen S, Lin C. High-performance bimetallic film surface plasmon resonance sensor based on film thickness optimization. Optik 2016;127:7514–9. https://doi.org/10.1016/j.ijleo.2016.05.085.
[15] Maurya J, François A, Prajapati Y. Two-dimensional layered nanomaterial-based one-dimensional photonic crystal refractive index sensor. Sensors 2018;18:857. https://doi.org/10.3390/s18030857.
[16] Zhu Y, Murali S, Cai W, Li X, Suk JW, Potts JR, et al. Graphene and graphene oxide: synthesis, properties, and applications. Adv Mater 2010;22:3906–24. https://doi.org/10.1002/adma.201001068.
[17] Schasfoort RBM, Tudos AJ, editors. Handbook of Surface Plasmon Resonance: Cambridge: Royal Society of Chemistry; 2008. 10.1039/9781847558220.
[18] Wu L, Chu HS, Koh WS, Li EP. Highly sensitive graphene biosensors based on surface plasmon resonance. Opt Express 2010;18:14395. 10.1364/OE.18.014395.
[19] Zeng S, Hu S, Xia J, Anderson T, Dinh X-Q, Meng X-M, et al. Graphene–MoS2 hybrid nanostructures enhanced surface plasmon resonance biosensors. Sens Actuators, B 2015;207:801–10. https://doi.org/10.1016/j.snb.2014.10.124.
[20] Ouyang Q, Zeng S, Jiang L, Hong L, Xu G, Dinh X-Q, et al. Sensitivity enhancement of transition metal dichalcogenides/silicon nanostructure-based surface plasmon resonance biosensor. Sci Rep 2016;6:28190. https://doi.org/10.1038/srep28190.
[21] Wu L, Guo J, Wang Q, Lu S, Dai X, Xiang Y, et al. Sensitivity enhancement by using few-layer black phosphorus-graphene/TMDCs heterostructure in surface plasmon resonance biochemical sensor. Sens Actuators, B 2017;249:542–8. https://doi.org/10.1016/j.snb.2017.04.110.
[22] Wu L, Jia Y, Jiang L, Guo J, Dai X, Xiang Y, et al. Sensitivity improved SPR biosensor based on the MoS2/graphene–aluminum hybrid structure. J Lightwave Technol 2017;35:82–7. https://doi.org/10.1109/JLT.2016.2624982.
[23] Zhao X, Huang T, Ping P, Wu X, Huang P, Pan J, et al. Sensitivity enhancement in surface plasmon resonance biochemical sensor based on transition metal dichalcogenides/graphene heterostructure. Sensors 2018;18:2056. https://doi.org/10.3390/s18072056.
[24] Verma A, Prakash A, Tripathi R. Sensitivity enhancement of surface plasmon resonance biosensor using graphene and air gap. Opt Commun 2015;357:106–12. https://doi.org/10.1016/j.optcom.2015.08.076.
[25] Rouf HK, Haque T. Performance enhancement of AG-AU bimetallic surface plasmon resonance biosensor using INP. PIER M 2018;76:31–42. https://doi.org/10.2528/PIERM18092503.
[26] Maharana PK, Jha R, Palei S. Sensitivity enhancement by air mediated graphene multilayer based surface plasmon resonance biosensor for near infrared. Sens Actuators, B 2014;190:494–501. https://doi.org/10.1016/j.snb.2013.08.089.
[27] Bijalwan A, Singh BK, Rastogi V. Surface plasmon resonance-based sensors using nano-ribbons of graphene and WSe2. Plasmonics 2020;15:1015–23. https://doi.org/10.1007/s11468-020-01122-w.
[28] Menon PS, Jamil NA, Mei GS, Zain ARM, Hewak D, Huang C-C, et al. Multilayer CVD-Graphene and MoS2 Ethanol sensing and characterization using Kretschmann-based SPR. IEEE J Electron Devices Soc 2020:1–1. 10.1109/JEDS.2020.3022036.
[29] Hasib MHH, Nur JN, Rizal C, Shushama KN. Improved transition metal dichalcogenides-based surface plasmon resonance biosensors. Condensed Matter 2019;4:49. https://doi.org/10.3390/condmat4020049.
[30] Malitson IH. A redetermination of some optical properties of calcium fluoride. Appl Opt 1963;2:1103. https://doi.org/10.1364/AO.2.001103.
[31] Sharma AK, Gupta BD. On the performance of different bimetallic combinations in surface plasmon resonance based fiber optic sensors. J Appl Phys 2007;101:093111. https://doi.org/10.1063/1.2721779.
[32] Maurya JB, Prajapati YK. A comparative study of different metal and prism in the surface plasmon resonance biosensor having MoS2-graphene. Opt Quant Electron 2016;48:280. https://doi.org/10.1007/s11082-016-0562-6.
[33] Mishra AK, Mishra SK, Verma RK. Doped single-wall carbon nanotubes in propagating surface plasmon resonance-based fiber optic refractive index sensing. Plasmonics 2017;12:1657–63. https://doi.org/10.1007/s11468-016-0431-y.
[34] Bruna M, Borini S. Optical constants of graphene layers in the visible range. Appl Phys Lett 2009;94:031901. https://doi.org/10.1063/1.3073717.
[35] Gedney SD, Zhao B. An auxiliary differential equation formulation for the complex-frequency shifted PML. IEEE Trans Antennas Propagat 2010;58:838–47. https://doi.org/10.1109/TAP.2009.2037765.
[36] Bérenger J-P. Perfectly matched layer (PML) for computational electromagnetics. Synth Lect Comput Electromag 2007;2:1–117. https://doi.org/10.2200/S00030ED1V01Y200605CEM008.
[37] Kim N-H, Choi M, Kim TW, Choi W, Park SY, Byun KM. Sensitivity and stability enhancement of surface plasmon resonance biosensors based on a large-area Ag/MoS2 substrate. Sensors 2019;19:1894. https://doi.org/10.3390/s19081894.
[38] Wang G, Wang C, Yang R, Liu W, Sun S. A sensitive and stable surface plasmon resonance sensor based on monolayer protected silver film. Sensors 2017;17:2777. https://doi.org/10.3390/s17122777.
[39] Srivastava A, Galande C, Ci L, Song L, Rai C, Jariwala D, et al. Novel liquid precursor-based facile synthesis of large-area continuous, single, and few-layer graphene films. Chem Mater 2010;22:3457–61. https://doi.org/10.1021/cm101027c.
[40] Elías AL, Perea-López N, Castro-Beltrán A, Berkdemir A, Lv R, Feng S, et al. Controlled synthesis and transfer of large-area WS_2 sheets: from single layer to few layers. ACS Nano 2013;7:5235–42. https://doi.org/10.1021/nn400971k.
[41] Wang H, Zhang H, Dong J, Hu S, Zhu W, Qiu W, et al. Sensitivity-enhanced surface plasmon resonance sensor utilizing a tungsten disulfide (WS 2) nanosheets overlayer. Photon Res 2018;6:485. https://doi.org/10.1364/PRJ.6.000485.
[42] Yu L, Lee Y-H, Ling X, Santos EJG, Shin YC, Lin Y, et al. Graphene/MoS_2 hybrid technology for large-scale two-dimensional electronics. Nano Lett 2014;14:3055–63. https://doi.org/10.1021/nl404795z.
[43] Maurya JB, Prajapati YK, Singh V, Saini JP. Sensitivity enhancement of surface plasmon resonance sensor based on graphene–MoS2 hybrid structure with TiO2–SiO2 composite layer. Appl Phys A 2015;121:525–33. https://doi.org/10.1007/s00339-015-9442-3.
[44] Tabasi O, Falamaki C. Recent advancements in the methodologies applied for the sensitivity enhancement of surface plasmon resonance sensors. Anal Methods 2018;10:3906–25. https://doi.org/10.1039/C8AY00948A.
[45] Hossain MdB, Tasnim T, Abdulrazak LF, Rana MdM, Islam MdR. A numerical approach to design the Kretschmann configuration based refractive index graphene-MoS2 hybrid layers with TiO2-SiO2 nano for formalin detection. Photonic Sens 2020;10:134–46. https://doi.org/10.1007/s13320-019-0566-5.
[46] Lopez-Sanchez O, Lembke D, Kayci M, Radenovic A, Kis A. Ultrasensitive photodetectors based on monolayer MoS2. Nature Nanotech 2013;8:497–501. https://doi.org/10.1038/nnano.2013.100.
[47] Hoggard A, Wang L-Y, Ma L, Fang Y, You G, Olson J, et al. Using the plasmon linewidth to calculate the time and efficiency of electron transfer between gold nanorods and graphene. ACS Nano 2013;7:11209–17. https://doi.org/10.1021/nn404985h.
[48] Kim J, Son H, Cho DJ, Geng B, Regan W, Shi S, et al. Electrical control of optical plasmon resonance with graphene. Nano Lett 2012;12:5598–602. https://doi.org/10.1021/nl302656d.
[49] Niu J, Jun Shin Y, Lee Y, Ahn J-H, Yang H. Graphene induced tunability of the surface plasmon resonance. Appl Phys Lett 2012;100:061116. https://doi.org/10.1063/1.3683534.
[50] Lee S, Lee M hyung, Shin H, Choi D. Control of density and LSPR of Au nanoparticles on graphene. Nanotechnology 2013;24:275702. 10.1088/0957-4484/24/27/275702.
[51] Reckinger N, Vlad A, Melinte S, Colomer J-F, Sarrazin M. Graphene-coated holey metal films: Tunable molecular sensing by surface plasmon resonance. Appl Phys Lett 2013;102:211108. https://doi.org/10.1063/1.4808095.
[52] Zaniewski AM, Schriver M, Gloria Lee J, Crommie MF, Zettl A. Electronic and optical properties of metal-nanoparticle filled graphene sandwiches. Appl Phys Lett 2013;102:023108. https://doi.org/10.1063/1.4772542.
[53] Johnson PB, Christy RW. Optical constants of the noble metals. Phys Rev B 1972;6:4370–9. https://doi.org/10.1103/PhysRevB.6.4370.
[54] Nur JN, Hasib MHH, Asrafy F, Shushama KN, Inum R, Rana MdM. Improvement of the performance parameters of the surface plasmon resonance biosensor using Al2O3 and WS2. Opt Quant Electron 2019;51:174. 10.1007/s11082-019-1886-9.